P5A.3 OBSERVATIONS OF THE FINESCALE STRUCTURE OF 11 JUNE DRYLINE DURING IHOP 2002

Huaqing Cai*
Advanced Study Program and Atmospheric Technology Division
National Center for Atmospheric Research, CO 80307

Wen-Chau Lee
Atmospheric Technology Division
National Center for Atmospheric Research, CO 80307

1. INTRODUCTION

The International H2O Project (IHOP 2002) is a multi-agency field campaign aimed at improving the understanding of the role of water vapor in various atmospheric processes such as convection initiation (CI). Both ground-based and airborne state-of-art remote sensing technologies are used to monitor the three dimensional kinematic and thermodynamic variations of the atmosphere in unprecedented high time and space resolution. It is well known that the ability to identify where and when convection will start is crucial in improving numerical weather forecast in the warm season. One major component of IHOP 2002 is trying to use all the available observational tools to reconstruct the 3D kinematic and water vapor fields and trying to understand why convection initiates in certain places at certain time.

It has been know for a long time that boundaries such as dryline are favorable places for convection initiation, however, not every dryline initiates storms. This paper presents a case study of a retrogressing dryline in Oklahoma Panhandle on 11 June 2002 during IHOP 2002. The major observational tools employed in this study include ELDORA airborne Doppler radar, Learjet dropsondes, NCAR mobile GLASS soundings, DRI microwave radiometers, NCAR S-POL radar as well as other conventional weather observations such as satellite imagery and surface observations. The dryline was associated with impressive cloud line (see Fig. 2) but failed to initiate storms inside the IHOP Intensive Observation Domain (IOD) where the aircraft and ground-based mobile crew were collecting data. Interestingly enough, convection was initiated both north and south of the IHOP IOD (see Fig. 1).

* *Corresponding auther address:* Huaqing Cai, ASP/ATD, National Center for Atmospheric Research, Boulder, CO 80307; e-mail: caihq@ucar.edu

2. LARGE SCALE ENVIRONMENT

Fig.1 shows the satellite imagery superimposed on surface analysis at 2230 UTC. The small box in the Oklahoma Panhandle represents the IHOP IOD. Surface analysis indicates there is a dryline pass across the IHOP IOD from southwest to northeast. The intensive observations inside the box lasted from 2100 to 2330 UTC. Sometimes there were impressive cloud lines near the dryline during this time period. Fig. 2 is radar reflectivity from ELDORA airborne Doppler radar at 21:13:39 UTC. This quasi-vertical cross section perpendicular to the dryline shows a single cell with maximum radar reflectivity of 17 dBZ. In contrast, the dryline itself has a radar reflectivity of 4 dBZ. The distance between the cloud line and the dryline is ~12 km, with the cloud being in the southeast of the dryline inside the warm moist airmass. The cloud line was almost parallel to the dryline and the cloud base is ~5 km AGL. Although there was no storm initiated inside the IHOP IOD, storm A (see Fig. 1) was initiated north of the IHOP

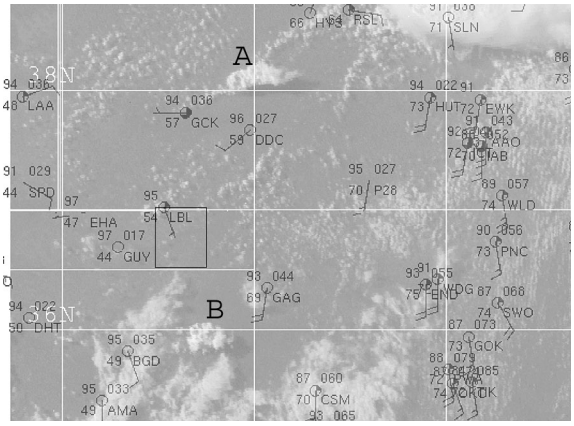

Fig. 1. Satellite imagery superimposed on surface analysis at 2230 UTC. The small box in the Oklahoma Panhandle represents the IHOP Intensive Observation Domain (IOD) from 2100 to 2330 UTC. A and B denote the two storms initiated around 2230 UTC.

IOD along a gust front associated with a very intense storm started earlier on that day and storm B was initiated south of IHOP IOD probably near the dryline. The reason the portion of the dryline inside the IHOP IOD was not able to initiate any storm was explored in Section 4 of this paper.

3. CROSS LINE VARIABILITY

The NRL-P3 was flying along the dryline most of the time but it did penetrate the dryline several times during the entire mission. Fig. 3 is an example of the cross line variability of some flight level data taken from P3. The water vapor mixing ratio in panel (a) shows a drop of ~3.0 g/kg when the aircraft passing the dryline from southeast side to northwest side. At the same time, virtual potential temperature increases less than 0.5 K while equivalent potential temperature drops ~10 K. Compared with past observational studies of drylines in the west Great Plains (Parsons et al. 1991; Atkins et al. 1998), the virtual potential temperature difference between the hot dry and warm moist airmass is rather small in this particular case. The small virtual potential temperature difference may also contribute to slow propagation speed of this dryline.

In addition to airborne observations from several aircraft, surface mobile Doppler radars (DOWs), mobile mesonet and mobile dual-channel microwave radiometer were also converged inside the IHOP IOD making various measurements. Fig. 4 shows the temperature, relative humidity, total precipitable water vapor and cloud liquid water across the dryline inside IHOP IOD measured by Desert Research Institute (DRI)'s dual-channel microwave radiometer. Just as we expected, temperature is warmer (~ 2

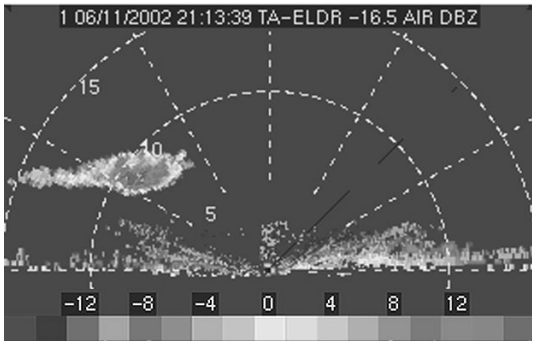

Fig. 2. Quasi-vertical cross section of radar reflectivity from the aft antenna of ELDORA airborne Dopper radar at 21:13:39 UTC. The cross section is almost perpendicular to the dryline and the radar is at the center of the azimuth spokes.

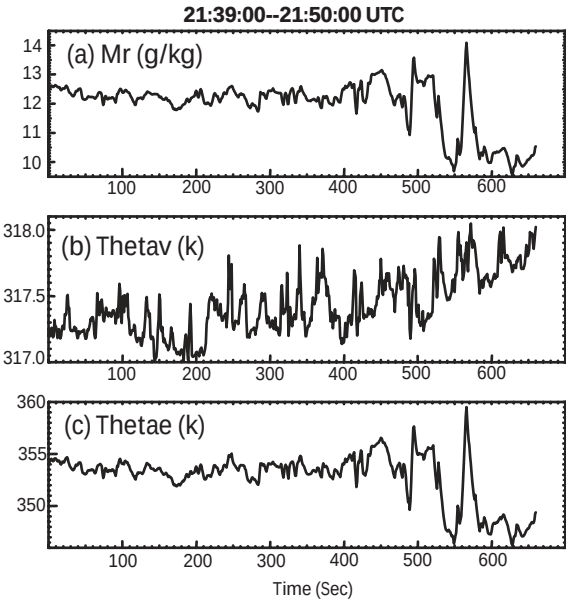

Fig. 3. Time series of NRL-P3 flight level data. (a) water vapor mixing ratio (g/kg); (b) virtual potential temperature (K); (c) equvalent potential temperature (K). The abscissa represents the time past 2139 UTC in seconds.

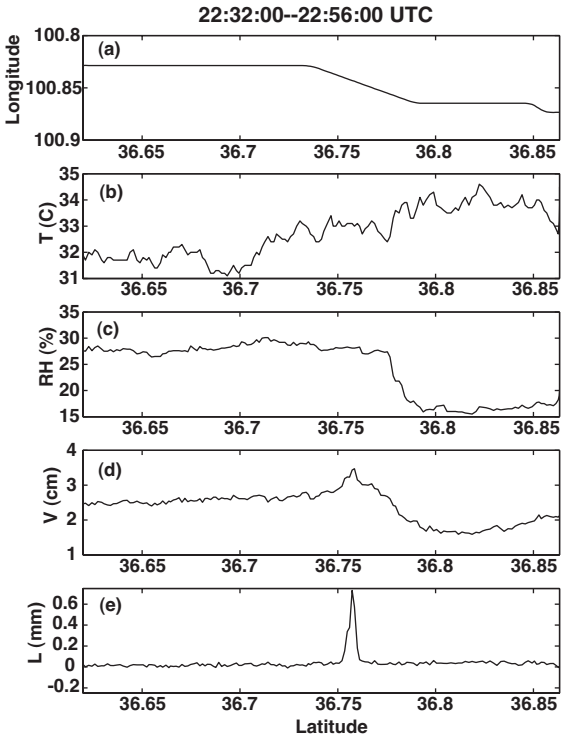

Fig. 4. A north-south transect through the dryline by DRI microwave radiometer. (a) the radiometer track; (b) temperature (°C); (c) relative humidity (%); (d) total precipitable water vapor (cm); (e) liquid water (mm). The abscissa represents latitude in degrees.

°C) on the northwest side of the dryline, the relative humidity is higher on the southeast side of the dryline. Notice both the total precipitable water vapor and could liquid water peaked about 2 km south of the surface dryline position. The cloud liquid water shows a sharp spike of 0.7 mm indicating a narrow cloud line with high liquid water content. The total precipitable water vapor difference on both side of the dryline is ~ 0.5 cm in the dryline environment and ~ 1.5 cm near the dryline. The moist convergence near the dryline shown in the total precipitable water vapor is most probably associated with the cloud line.

The vertical structure of the hot dry and warm moist airmass on both side of the dryline is represented by the NCAR mobile soundings taken at 2051 UTC ~2 km southeast of the dryline and at 2137 UTC ~11 km northwest of the dryline (Fig. 5). The dry air is slightly hotter than the moist air up to until 700 mb (3.1 km MSL). The inversion near 650 mb (3.7 km MSL) on the moist side is stronger than that on the dry side. The moist air on both side of the boundary extends up to 700 mb (3.1 km MSL) with the dew point temperature being ~6 °C greater on the moist side. There is a substantial dry layer from 700 mb (3.1 km MSL) to 500 mb (5.9 km MSL) on both side of the dryline. The moist layer starting from 500 mb (5.9 km MSL) is corresponding to the layer

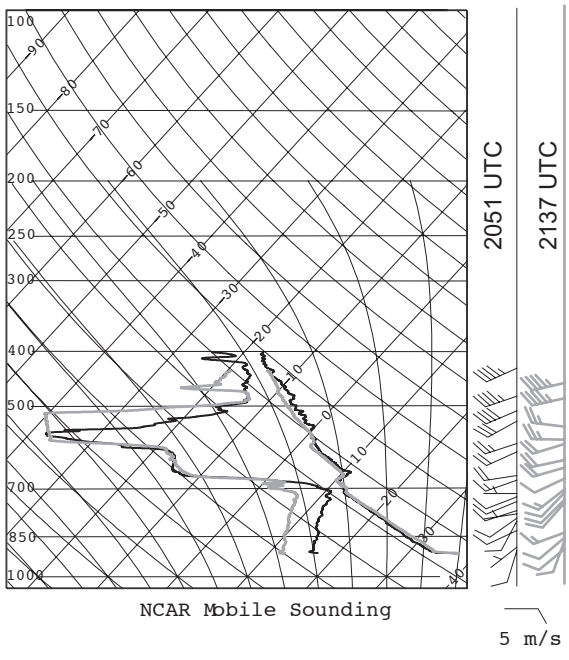

Fig. 5. NCAR mobile sounding at 2051 UTC (black lines) and 2137 UTC (gray lines). The 2051 sounding is in the warm moist airmass while the 2137 sounding is in the hot dry airmass.

where the cloud line is embedded. Winds are relatively weak (~ 5 m/s) at lower levels and there is no apparent wind shift associated with the surface dryline. The Level of Free Convection (LFC) for a surface based air parcel is estimated to be 3.3 and 4.4 km MSL for the warm moist and hot dry airmass, respectively. It is possible that the inversion around 650 mb (3.7 km MSL) and the dry layer from 700 mb (3.1 km MSL) to 500 mb (5.9 km MSL) might contribute to the inability of the dryline initiating storms.

4. DETAIL KINEMATIC STRUCTURE OF THE DRYLINE

The clear air capability of ELDORA has been demonstrated by Wakimoto et al. (1996) and Atkins et al. (1998). On 11 June 2002 between 2100-2330 UTC there were 8 legs executed by NRL-P3 along the dryline inside the IHOP IOD indicated by the small box in Fig. 1. An example of the averaged vertical cross section perpendicular to the dryline is shown in Fig. 6. The dryline was estimated moving from 138° at a speed of 2.5 m/s by using consecutive S-Pol radar reflectivity data. Fig. 6a indicates a tilting of the radar reflectivity maximum toward the hot dry airmass which is consistent with previous dryline observations (Atkins et al. 1998).

The updraft maximum occurred at ~ 2.5 km AGL with a value of 0.75 m/s, which is pretty weak but close to the Level of Free Convection (LFC) of 3.3 km MSL (~2.5 km AGL) in the moist airmass obtained from NCAR mobile soundings (see Fig. 5). It should be pointed out that the LFC of 3.3 km MSL was estimated based on a surface air parcel, which might not reach the LFC in this case. Trajectory analysis will be needed to find out how high a surface parcel can go. It is hypothesized that the inversion layer around 650 mb, the dry layer from 700 mb to 500 mb and the weak lifting from the dryline itself contribute to the lack of convection initiation inside IHOP IOD.

5. DISCUSSIONS AND FUTURE WORK

The detailed kinematic structure of the 11 June 2002 dryline has been documented by ELDORA observations. Future work will concentrate on the analysis of the Learjet dropsonds, S-Pol radar refractive index and Leandre water vapor data to obtain a complete picture of moisture field associated with the dryline. Detailed kinematic and moisture fields of the dryline will help us to understand why this particular portion of the dryline failed to initiate storms.

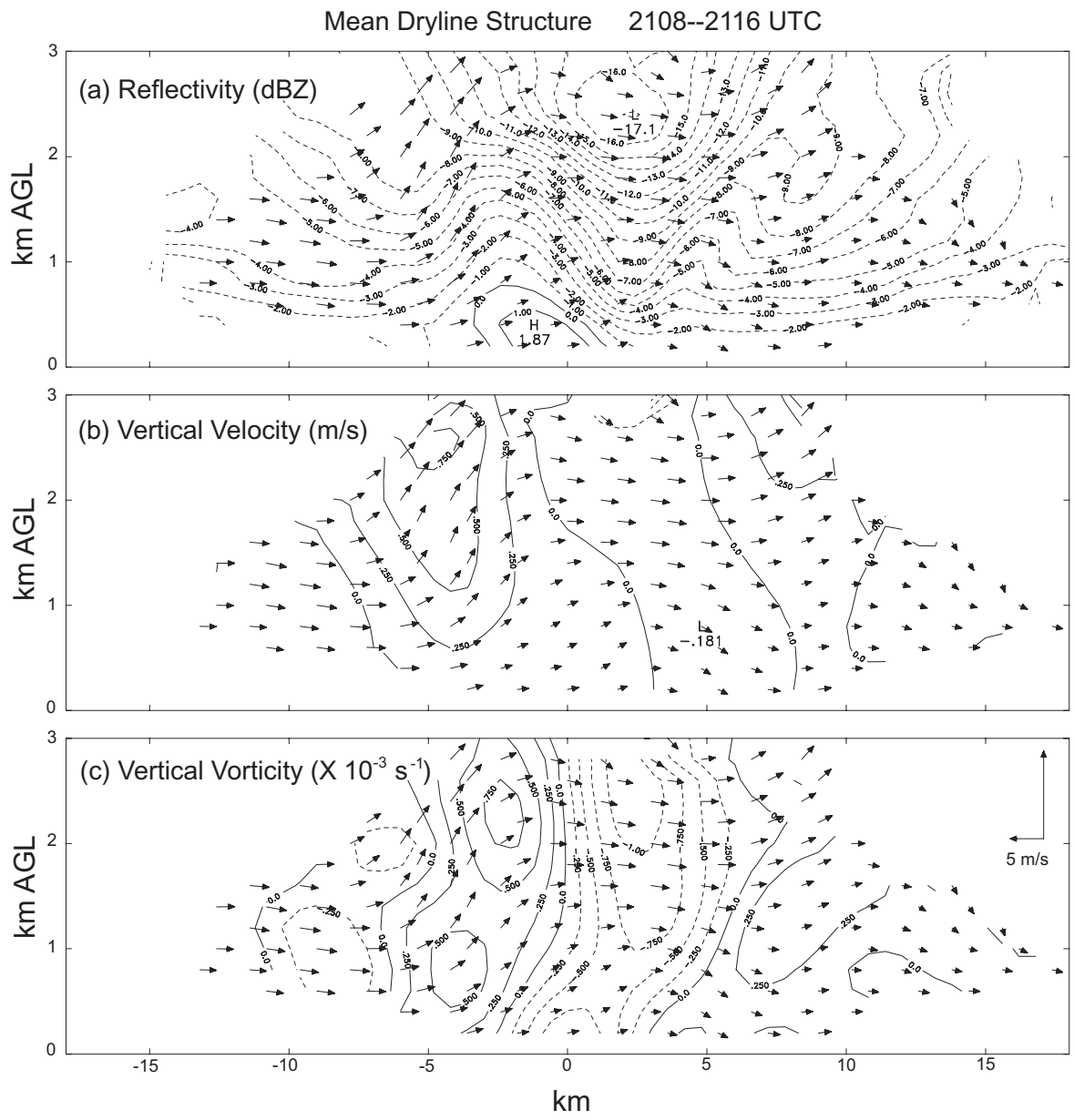

Fig. 6. Averaged vertical cross section of (a) radar reflectivity (dBZ); (b) vertical velocity (m/s) and (c) vertical vorticity (10^{-3} s^{-1}) for 11 June 2002 dryline during IHOP 2002. Dryline-relative wind vectors are superimposed on each panel.

REFERENCES

Atkins, N. T., R. M. Wakimoto and C. L. Ziegler, 1998: Observations of the finescale structure of a dryline during VORTEX 95. *Mon. Wea. Rev.*, **126**, 525-550.

Parsons, D. B., M. A. Shapiro, R. M. Hardesty, R. J. Zamora, and J. M. Intrieri, 1991: The finescale structure of a west Texas dryline. *Mon. Wea. Rev.*, **119,** 1283-1292.

Wakimoto, R. M., W.-C. Lee, H. B. Bluestein, C.-H. Liu, and P. H. Hildebrand, 1996: ELDORA observations during VORTEX 95. *Bull. Amer. Meteor. Soc.,* **77,** 1465-1481.